THE JOURNAL OF BIOLOGICAL CHEMISTRY
Vol. 278, No. 20, Issue of May 16, pp. 18455–18463, 2003
Printed in U.S.A.

The Protein Complex Composed of Nickel-binding SrnQ and DNA Binding Motif-bearing SrnR of *Streptomyces griseus* Represses *sodF* Transcription in the Presence of Nickel*

Received for publication, November 18, 2002, and in revised form, February 27, 2003
Published, JBC Papers in Press, March 17, 2003, DOI 10.1074/jbc.M211740200

Ju-Sim Kim‡, Sa-Ouk Kang§, and Jeong K. Lee‡¶

From the ‡Department of Life Science, Sogang University, Seoul 121-742, Korea and the §School of Biological Sciences, Institute of Microbiology, Seoul National University, Seoul 151-742, Korea

Nickel-responsive transcriptional repression of *sodF*, which codes for iron- and zinc-containing superoxide dismutase of *Streptomyces griseus*, was mediated through an operator (−2 to +15) spanning over the 5′ end (+1) of the transcript. Two open reading frames, SrnR (12,343 Da) and SrnQ (12,486 Da), with overlapping stop-start codons were identified downstream from *sodF* and found responsible for the repression of *sodF*. The deduced amino acid sequence of SrnR revealed a DNA binding motif and showed homology to the transcriptional regulators of ArsR family, whereas SrnQ did not show any similarity to any known proteins. When *srnRQ* DNA was maintained *in trans* in *S. griseus* on a multicopy plasmid, *sodF* transcription was highly repressed by nickel, but neither *srnR* nor *srnQ* alone showed the effect. Consistently, the *sodF* transcription of *srnR*-interrupted mutant was no longer repressed by nickel, which was complemented only with *srnRQ* DNA. Nickel-dependent binding of SrnR and SrnQ to the *sodF* operator DNA was observed only when the two proteins were provided together. The maximum protein-DNA interaction was shown when SrnR and SrnQ were present in one-to-one stoichiometric ratio. The two proteins appear to constitute an octamer composed of four subunits of each protein. SrnR directly interacted with SrnQ, and the protein interaction did not require nickel. The conformation of SrnQ was changed upon nickel binding, which was in the ratio of one Ni^{2+} ion per protein molecule. A model is proposed in which SrnQ of the protein complex senses nickel and subsequently enhances the DNA binding activity of SrnR through the protein-protein interaction.

Aerobic organisms have acquired a specific mechanism to protect themselves from reactive oxygen species (ROS)[1] such as superoxide radical (O_2^-) and hydrogen peroxide (H_2O_2), which can be generated from incomplete reduction of dioxygen during respiration. The ROS may cause oxidative damage to DNA, protein, and lipid (1). The Fenton reaction generating hydroxy radicals by reduction and oxidation of Fe ions in the presence of ROS has been proposed as a mechanism for cell damage (2). Major defense system against ROS comprises superoxide dismutase (SOD), catalase, and peroxidase, which concertedly convert the ROS into O_2 and H_2O (3). The SOD is distinguished into several types according to their active metals (2). The SOD containing either manganese (Mn-SOD) or iron (Fe-SOD) has been found in the cytoplasm of prokaryotic cells. The copper- and zinc-containing SOD (CuZn-SOD) has been described in the periplasm of several bacteria (4–6). In addition, two novel SODs containing nickel (Ni-SOD) or both iron and zinc (FeZn-SOD) have been characterized as cytoplasmic enzymes of *Streptomyces griseus* and *Streptomyces coelicolor* (7, 8).

The Ni-SOD and FeZn-SOD are found as homotetramers of approximately 13- and 22-kDa subunits, respectively, in *S. griseus* (7) and *S. coelicolor* (8). The expression of *sodN* coding for Ni-SOD of *S. coelicolor* (9) and *S. griseus*[2] increased in the presence of nickel, whereas their FeZn-SOD (*sodF*) expressions were regulated through the repression of *sodF* transcription in the presence of nickel (10, 11). Previously, we found that the nickel-responsive transcriptional repression of *sodF* of *S. griseus* was exerted through an inverted-repeat sequence ($TT\boldsymbol{G}CAN_7TGCAA$) overlapping the 5′ end (+1, ***G***) of *sodF* transcript (11). In addition, nickel-dependent interaction between cell extracts and the *sodF* operator DNA was confirmed by gel-mobility shift assay (11), suggesting the presence of trans-acting regulatory protein(s) responsible for the repression. To the best of our knowledge, a nickel-responsive transcriptional regulator has not been described in Gram-positive bacteria, whereas a transcriptional regulator, NikR, has been found for the repression of *nik* operon coding for ATP-dependent nickel transport system of *Escherichia coli* when nickel is provided in excess (12). An inverted-repeat sequence in the promoter of *nik* operon was proposed as a potential NikR-binding site (13, 14). No sequence homology was found between the inverted-repeat sequence of *E. coli nik* operon and the operator of *S. griseus sodF* gene.

In this study, we identified *srnRQ* coding for two small proteins mediating nickel-responsive transcriptional repression of *S. griseus sodF* (*srn* stands for sodF repression by nickel). They are located immediately downstream from *sodF*. SrnR and SrnQ appear to form an octameric complex composed of four subunits of each protein and then bind to the *sodF* operator in a nickel-responsive manner. We propose that DNA binding motif-bearing SrnR is a repressor, whereas nickel-binding SrnQ is a co-repressor. A hypothetical model for the

* The costs of publication of this article were defrayed in part by the payment of page charges. This article must therefore be hereby marked "*advertisement*" in accordance with 18 U.S.C. Section 1734 solely to indicate this fact.

The nucleotide sequence(s) reported in this paper has been submitted to the GenBank™/EBI Data Bank with accession number(s) AF1418663.

¶ To whom correspondence should be addressed: Dept. of Life Science, Sogang University, Mapo, Shinsu 1, Seoul 121-742, Korea. Tel.: 82-2-705-8459; Fax: 82-2-704-3601; E-mail: jgklee@ccs.sogang.ac.kr.

[1] The abbreviations used are: ROS, reactive oxygen species; SOD, superoxide dismutase; Sm, streptomycin; Sp, spectinomycin; Km, kanamycin; Apr, apramycin; GST, glutathione *S*-transferase; ORF, open reading frame; XylE, cathechol dioxygenase; IPTG, isopropyl-1-thio-β-D-galactopyranoside; Tricine, *N*-[2-hydroxy-1,1-bis(hydroxymethyl)ethyl]glycine.

[2] J.-S. Kim and J. K. Lee, unpublished results.

repression of *sodF* transcription by the SrnR·SrnQ complex is presented.

EXPERIMENTAL PROCEDURES

Bacterial Strains and Growth Conditions—*S. griseus* ATCC 23345 was grown at 28 °C in YEME or YMPD medium as described previously (15, 16). *S. griseus* protoplast was prepared as described previously (15, 17) and used for transformation with plasmid DNA, which was isolated from *E. coli* SURE strain (Stratagene) (18). Transformants were selected on R2YE agar plate (15). Ampicillin, streptomycin (Sm), spectinomycin (Sp), kanamycin (Km), and apramycin (Apr) (final concentrations of 50, 25, 25, 25, and 50 μg/ml, respectively) were used when *E. coli* carried the antibiotic-resistant genes. Km, Apr, and thiostrepton were used at 5, 5, and 20 μg/ml, respectively, when appropriate for *S. griseus* culture.

Nucleotide Sequence Accession Number—Nucleotide sequence of 0.86-kb *Sma*I/*Sal*I DNA (Fig. 1), which includes *srnRQ* of *S. griseus*, has been assigned to GenBank™ under the accession number AF1418663.

DNA Mutagenesis and Plasmid Construction—The initiation codon of SrnR and SrnQ were mutated by PCR including overlap extension as described previously (19). The 1.0-kb *Pst*I/*Sal*I DNA fragment containing *srnRQ* (Fig. 1) was cloned into pBS (Stratagene) to generate pBSRQ and used as a DNA template. The primer 5′-TGCACCCTTGGAATCAC-3′ (A of SrnR ATG codon was replaced by T) was used for the disruption of initiation codon of SrnR, whereas the SrnQ initiation codon was mutated using the primer 5′-CCTCATAGTCAGGCCT-3′ (AG was substituted for GA corresponding to the third (G) and first base (A) of the first and second codons of SrnQ, respectively, leaving the SrnR stop codon, originally TGA, as TAG). The PCR products were confirmed for the mutations through the DNA sequence analyses followed by digestion with *Pst*I and *Sal*I and cloning into *Pst*I/*Sal*I sites of pFD666 (20) to generate pFDR$^-$Q and pFDRQ$^-$ carrying the mutations in *srnR* and *srnQ*, respectively. Plasmid pFDRQ, also a derivative of pFD666, contained the same 1.0-kb *Pst*I/*Sal*I DNA including the wild-type *srnRQ* (Fig. 1).

Plasmid pIJK365 derived from a low copy number plasmid pXE4 (21) has the *sodF* regulatory DNA from −365 to +59 (+1, 5′ end of *sodF* transcript), which was transcriptionally fused to promoterless *xylE* DNA (11). pIM5in(+8+9) carries the same *sodF* DNA as in pIJK365 with the exception that a 5-bp nonspecific DNA was inserted between the left and right halves of the dyad symmetry (11). All plasmids contain transcription-translation stop Ω DNA (Sm^r/Sp^r) (22) upstream from the *sodF* DNA to block any fortuitous transcriptional read-through originated from the vector DNA.

Detection of Catechol Dioxygenase Activity—*S. griseus* containing *xylE* fusion plasmids were cultured for 48 h on an YEME agar plate. Cells were broken by sonication, and catechol dioxygenase activity was measured with cell extracts as described previously (21).

Detection of SOD Activity, Preparation of SOD, and Western Immunoblot Analysis—Activity staining of SOD in a native polyacrylamide (10%) gel was performed as described previously (23). The FeZn-SOD of *S. griseus* was purified and used as an immunogen to raise an antiserum from mouse as described previously (7). The preparation of cell extracts, electrophoresis (SDS-PAGE, 15% polyacrylamide), and electroblotting of proteins were also performed according to the methods as described previously (7, 24). A blot treated with FeZn-SOD-specific antibody was reacted with a 1/5000 dilution of goat anti-mouse IgG (Pierce) conjugated with horseradish peroxidase, which was visualized using an ECL detection system supplied by Amersham Biosciences (11). Protein was determined by a modified Lowry method using bovine serum albumin (Sigma) as a standard (25). The relative SOD activities and FeZnSOD protein levels between samples were quantified by scanning the gel and blot with Tina 2.0 program of a BIO-Imaging analyzer (Fuji).

Expression of SrnR and SrnQ in E. coli—pBSRQ has an insert of the 1.0-kb *Pst*I/*Sal*I DNA containing *srnRQ* (Fig. 1) in the same orientation as *lac* promoter of pBS. pBSR$^-$Q and pBSRQ$^-$ harbored the same insert DNA as in pBSRQ with the exception of mutations in initiation codon of SrnR and SrnQ, respectively. Plasmids pBSRQ, pBSR$^-$Q, and pBSRQ$^-$ were transformed into *E. coli* DH5α. Expression of SrnR and SrnQ was induced by IPTG at 0.1 mM for 2 h after A_{600} of *E. coli* culture reached 0.6–0.7. SrnR and SrnQ were separated using Tricine-SDS-PAGE (26). The separating gel of 16.5% T, 6% C was overlaid with a 4% T, 3% C stacking gel (T denotes the total percentage concentration of both acrylamide and bisacrylamide, and C is the percentage concentration of bisacrylamide relative to the total concentration).

Gene Disruption—A partially digested *Bam*HI fragment of 4.2 kb containing *sodF* and *srnRQ* (Fig. 7) was cloned into pKC1139 (Apr^r) (27), which has a temperature-sensitive replication origin to generate pKCR. The *Eco*N1 site within *srnR* of the plasmid was interrupted through ligation with 2.2-kb transcription-translation stop Ω DNA (Km^r) (28) following end flushing with Klenow fragment. The resulting plasmid pKCRKm was introduced into *S. griseus*, and transformants were selected on YMPD agar plate containing Km and Apr at 28 °C. Single cross-over recombinants (Km^r and Apr^r) were obtained after incubation of the transformant at 37 °C. The spores of single cross-over then were grown in YMPD broth without Apr for 72 h and plated on to the same medium containing Km. Kanamycin-resistant colonies thus obtained were examined for their sensitivity to Apr, and finally, three colonies showing Km^r and Apr^s, which were regarded as *srnR*-interrupted mutants, were selected among approximately 50 colonies. All of the mutants were confirmed for their chromosomal arrangements of disruptions by Southern hybridization with probes labeled with [α-^{32}P]dCTP using DNA-labeling beads (Amersham Biosciences), and one *srnR* disruptant, R45, was chosen for further analyses.

RNA Isolation, Quantification, and Northern (RNA) Hybridization Analysis—Total RNA was extracted from *S. griseus* as described previously (29). RNA quantification, electrophoretic separation of denatured RNA, blot transfer, labeling of strand-specific RNA probe using [α-^{32}P]CTP, and hybridization with the probe were performed as described previously (11, 30). Transcript levels were quantified by densitometer scan of the resulting autoradiograms with the BIO-Imaging analyzer.

Overexpression and Purification of SrnR and SrnQ Using Fusion to Glutathione S-Transferase (GST)—To clone *srnR* and *srnQ* into GST fusion plasmid pGEX-5X-3 (Amersham Biosciences), initiation and stop codons of the genes were modified to have *Bam*HI and *Xho*I sites, respectively. An N-terminal primer, 5′-AACATGCAC**GGATCC**AATCACGCGCC-3′ (mutated sequence *underlined* unless otherwise noted), with the SrnR start codon changed into *Bam*HI site (in *boldface*) was used in PCR with a C-terminal primer, 5′-GAGGCCTGAT**CTCGAG**GCGTCGCC-3′, containing *Xho*I site (in *boldface*) mutated from the SrnR stop codon. For *srnQ*, an N-terminal primer, 5′-GGCGACGCC**GGATCC**TCAGGCCTCG-3′ (*Bam*HI site in *boldface*), and a C-terminal primer, 5′-CGCGCGGCCGT**CTCGAG**CCGGGTAGATC-3′ (*Xho*I site in *boldface*), were used. pBSRQ was used as a template. The PCR products were digested with *Bam*HI and *Xho*I and cloned into the expression vector pGEX-5X-3 to generate pGEXR and pGEXQ for the expression of SrnR and SrnQ, respectively. Sequence analyses confirmed the in-frame insertion into the plasmid as well as no other mutation in the amplified DNA.

When *E. coli* DH5α containing either pGEXR or pGEXQ grew up to A_{600} between 0.6 and 0.7, IPTG was added at 0.1 mM for overexpression of GST-SrnR and GST-SrnQ proteins. The cells were harvested at 2 h after IPTG induction, disrupted by sonication, and centrifuged at 4 °C to obtain cell-free extracts. The GST fusion proteins of ~39 kDa were identified by SDS-PAGE (12% polyacrylamide). The fusion proteins were purified from the cell lysate using glutathione-Sepharose 4B (Amersham Biosciences) followed by elution and concentration of native SrnR and SrnQ after the removal of GST by Factor Xa (New England Biolabs) digestion. The purified proteins were assessed for the purity and size by SDS-PAGE (15% polyacrylamide) (data not shown). The purified SrnR and SrnQ were used as immunogens to raise antisera as described previously (7).

Gel-mobility Shift Assay—The DNA fragments to be run for the assay were labeled with [γ-^{32}P]ATP using T4 polynucleotide kinase (Promega). The DNA probes (~10^4 cpm) were incubated at 25 °C with the varying amounts of the purified proteins of SrnR and/or SrnQ in the binding reaction buffer as described previously (11, 31). After a 10-min incubation with or without nickel, the reaction mixture was examined using 5% non-denaturing polyacrylamide gel as described previously (11). The results provided in this work are typical ones of at least three to four independent experiments showing virtually the same patterns.

Far-Western Immunoblot Analysis—Interaction between SrnR and SrnQ was analyzed as described previously (32). Native or SDS-heat-denatured (95 °C for 5 min in 0.2% SDS) SrnR (2 and 5 pmol) was prepared in TDGT buffer (50 mM Tris-HCl, pH 7.9, 0.15 mM NaCl, 1 mM dithiothreitol, 5% glycerol, and 0.05% Tween 20) with or without nickel followed by spotting onto nitrocellulose membrane. The nickel was used twice as much as the protein concentration. The blots were dried at room temperature for 1 h. After soaking in phosphate-buffered saline (24) containing 5% nonfat milk at room temperature for 30 min, blots were incubated in the same buffer containing native SrnQ (15 nM) for 1 h. After washing with phosphate-buffered saline three times, the

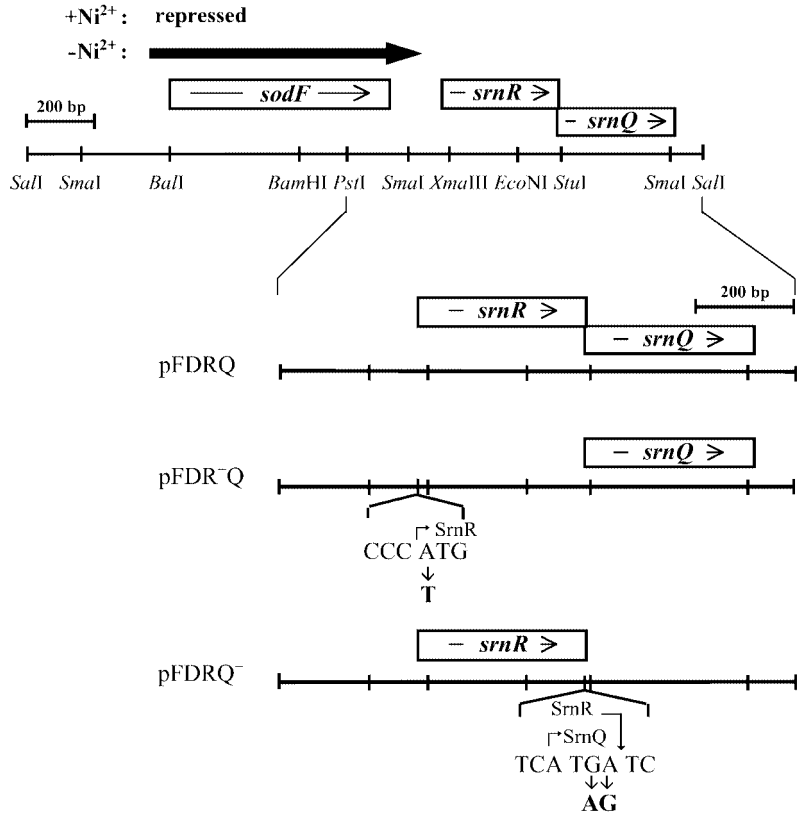

FIG. 1. ***S. griseus sodF* and its downstream DNA including *srnR* and *srnQ*.** The *sodF* transcription with respect to nickel is shown. Mutated nucleotides in start and stop codons of *srnRQ* are indicated in *boldface*. Plasmid pFDRQ contains the 1.0-kb *Pst*I/*Sal*I DNA fragment containing wild-type *srnRQ*. pFDR⁻Q and pFDRQ⁻ are identical to pFDRQ with the exception of the mutations.

membranes were treated with SrnQ-specific mouse antibodies in the same buffer, reacted with goat anti-mouse IgG conjugated with horseradish peroxidase, and detected with an ECL detection system (Amersham Biosciences).

Analytical Gel-filtration Chromatography—The complex of SrnR·SrnQ was identified through analytical Sephadex G-100 (Sigma) column (1.2 × 20.0, inner diameter × height (in cm)). The column buffer was 50 mM Tris-HCl, pH 7.5, containing 100 mM KCl (33). SrnR and SrnQ (60 μg each) were incubated at 25 °C for the protein interaction in the binding reaction buffer, which is the same as that used in the gel-mobility shift assay. The incubation continued with or without nickel (20 μM) for 10 min, and the samples were subjected to the column chromatography, which was run at room temperature. The A_{280} of the eluted fractions was measured, and SrnR and SrnQ in elutes were quantified using Tricine-SDS-PAGE (26).

CD Spectroscopy—Either SrnR or SrnQ (15 μM) was incubated at 25 °C in 10 mM Hepes, pH 7.6, containing 100 mM NaCl (14) with or without nickel (20 μM). The CD spectra of the proteins were obtained in wavelength range between 200 and 250 nm at 0.1-nm intervals with J-720 CD spectropolarimeter (Jasco). Five spectra with a resolution of 1 nm, a scan speed of 50 nm/min, and a response time of 1 s were averaged. The mean residue ellipticity was calculated using the molecular mass of each protein.

Nickel Binding Assay—Nickel binding of SrnQ and SrnR was assayed by atomic absorption spectrophotometry following equilibrium dialysis. 2-ml solution of SrnQ or SrnR (6.4 μM) was dialyzed against 0.5-liter buffer (10 mM Hepes, pH 7.6, 100 mM NaCl) (14) containing different amounts of $NiCl_2$ at 4 °C for 48 h. Unbound nickel was then removed by dialysis in ~500-fold volume of the 10 mM Hepes, pH 7.6, at 4 °C for 6 h. Metal content was determined with an AA-880 mark II atomic absorption (flame) spectrophotometer from Thermo Jarrel Ash. Each reading reported by the instrument was an average of three determinations. Bovine serum albumin was used as a control.

RESULTS

Nickel-dependent Expression of S. griseus FeZn-SOD Was Severely Repressed by the Multicopy Presence of the 1.0-kb DNA Downstream from sodF—The activity and protein level of FeZn-SOD were found much more repressed by nickel when the 1.0-kb *Pst*I/*Sal*I DNA (Fig. 1) downstream from *sodF* was maintained in multiple copies in cells (Fig. 2, *pFDRQ*). *S. griseus* harboring pFDRQ containing the *sodF* downstream DNA was grown on YEME agar plates supplemented with nickel up to 5 μM, and the FeZn-SOD activity and the protein level were measured at 48 h after inoculation. Although the FeZn-SOD expression of *S. griseus* having vector DNA, pFD666, decreased in proportion to nickel concentration (Fig. 2, *pFD666*), the presence of pFDRQ in repeated analyses always lowered the enzyme expression to a greater extent to display the activity (Fig. 2*A*) and the protein level (Fig. 2*B*) that are barely detectable at 5 μM nickel.

The sodF Downstream DNA Contains Two ORFs, SrnR and SrnQ—A sequence analysis of the *sodF* downstream DNA revealed two ORFs, which are oriented in the same direction as *sodF*, and started at 160 and 501 bp downstream from the SodF stop codon, respectively (Fig. 1). The first ORF (SrnR) consisted of 114 deduced amino acids with molecular mass of 12,343 Da, whereas the second ORF (SrnQ) revealed 110 amino acids of 12,486 Da. The initiation codon of SrnQ overlaps the stop codon of SrnR. A comparison of amino acid sequence between residues 12 and 82 of SrnR with data base revealed its homology to the transcriptional regulators of ArsR family (Fig. 3): ~61% similarity (33% identity) to HlyU, which up-regulates the transcription of hemolysin gene of *Vibrio cholerae* (34); 60% similarity (36% identity) to ArsR as a transcriptional repressor of the arsenical resistance genes of *Staphylococcus xylosus* (35); 59% similarity (36% identity) to the NolR involved in negative control of the expression of nodulation genes of *Rhizobium meliloti* (36); 57% similarity (40% identity) to MerR acting as an activator-repressor protein involved in mercury resistance of *Streptomyces lividans* (37); and 52% similarity (42% identity) to a putative ArsR found in genome data base of *S. coelicolor* M145 at Sanger center (www.sanger.ac.uk/Projects/S_coelicolor/). Around the middle of SrnR was found a putative helix-turn-helix motif as depicted in Fig. 3. No protein displaying homology to SrnQ was found. SrnQ has remarkably high content (26%) of arginine.

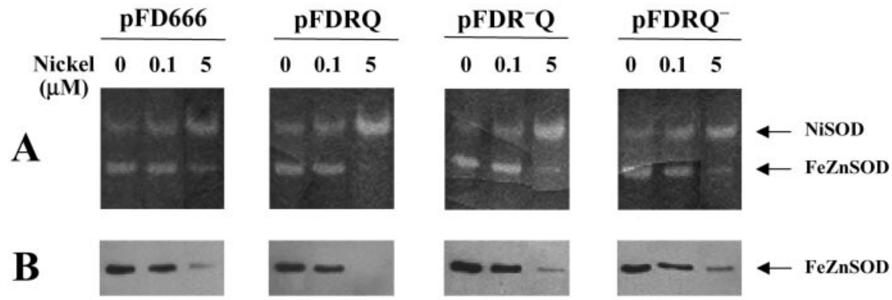

FIG. 2. **FeZnSOD expression of *S. griseus* containing *srnR* and *srnQ in trans*.** *S. griseus* harboring pFD666, pFDRQ, pFDR$^-$Q, or pFDRQ$^-$ was grown on YEME agar plates supplemented with nickel (0, 0.1, or 5 μM) for 48 h. Cell extracts were prepared through sonication. *A*, activity staining of SOD was done with 20 μg of protein/lane in 10% native polyacrylamide gel. *B*, Western immunoblot analysis of FeZnSOD was accomplished with 7 μg of protein/lane.

```
S.griseus    SrnR(114): 12-ASAFRALADPTRRQILEDLRG-GELAAGEIAGRFPISAPSISRHLGVLKGAGLVTERRDANRILYSLAEERL-82
V.cholerae   HlyU(108): 22-VVLLKAMANERRLQILCMLLD-NELSVGELSSRLELSQSALSQHLAWLRRDGLVNTRKEAQTVFYTLSSTEV-92
S.xylosus    ArsR(104):  7-STILKVLSDPSRLEILDLLSC-GELCACDLLEHFQFSQPTLSHHMKSLVDNELVTTRKNGNKHMYQLNHEFL-77
R.meliloti   NolR(122): 24-AGFLSAMANPKRLLILDSLVK-EEMAVGALAHKVGLSQSALSQHLSKLRAQNLVSTRRDAQTIYYSSSSDAV-94
S.lividans   MerR(125): 24-ARFFRALADPTRLKLLQFILR-GERTSAECVEHAGISQPRVSVHLSCLVDCGYVSARRDGKKLRYSVGDPRV-94
S.coelicolor ArsR(111): 12-ARFGRALADPIRCRILLTLRE-APAYPADLAEALQISRTRLSNHLACLRDCGLVVTVPDGRRSRYELADERL-82
                            • ••••••••  *• •*   •    •••  •••••    •*•• •* *•  *•• ••* •••••    *••  •••
```

helix-turn-helix

FIG. 3. **Sequence comparison of *S. griseus* SrnR with bacterial homologues.** Deduced amino acid sequence from residues 12–82 of SrnR was shown, and the sequence alignment was obtained using the ClustalW, version 1.80, program. Fully conserved residues are indicated with *asterisks*, whereas similar amino acids are marked with *dots*. The helix-turn-helix motif is indicated. The size of each protein is denoted by *residue number* in *parenthesis*, and the residue locations are shown with numbers on each side of the sequence.

Both SrnR and SrnQ Are Required for the Repression of FeZn-SOD Expression in the Presence of Nickel—To determine which ORF(s) of the *sodF* downstream DNA mediates the enhanced repression of FeZn-SOD in the presence of nickel, SrnR and SrnQ were mutagenized through PCR. As illustrated in pFDR$^-$Q (Fig. 1), the initiation codon of SrnR was changed into TTG resulting in SrnR$^-$. The SrnR mutation might have polar effect on the expression of downstream SrnQ, so the 213-bp *Xma*III-*Eco*NI DNA corresponding to the peptide from residues 9–78 of SrnR was in-frame deleted to generate pFD(ΔR)Q (data not shown). In addition, plasmid pFDRQ$^-$ was constructed to have a substitution of ATA for the initiation codon of SrnQ, but the SrnR stop codon, originally TGA, was still kept as TAG (Fig. 1).

The FeZn-SOD expression of *S. griseus* harboring either pFDR$^-$Q or pFDRQ$^-$ *in trans* was compared with that of the control cells containing pFD666 in the presence of nickel (Fig. 2). No significant difference in FeZn-SOD expression was observed. *S. griseus* having pFD(ΔR)Q showed the same results as those of the cells harboring pFDR$^-$Q (data not shown), suggesting no polar mutation for the expression of SrnQ by the SrnR$^-$ mutation of pFDR$^-$Q. Thus, the results clearly indicate that SrnR and SrnQ are required together for the *in trans* effect of the downstream DNA in multicopies.

SrnR and SrnQ Are Expressed in E. coli—It was examined whether *srnR* and *srnQ* code for the proteins of deduced sizes. The proteins were expressed through IPTG induction from *E. coli* harboring pBSRQ, pBSR$^-$Q, and pBSRQ$^-$. The orientation of *srnRQ* in these plasmids was the same as that of *lac* promoter, but their reading frames were shifted from that of the LacZ α-polypeptide of the plasmid. The Tricine-SDS-PAGE of the cell extracts of *E. coli* containing pBSRQ revealed two discrete polypeptides of ~12 kDa only after IPTG induction (Fig. 4, *lane 4*). The slow-moving band was regarded as SrnQ, because it was still detected with pBSR$^-$Q (Fig. 4, *lane 6*). The other fast-moving one was concluded to be SrnR because it was observed with pBSRQ$^-$ (Fig. 4, *lane 8*). The sizes of the expressed polypeptides were also similar to the deduced values of

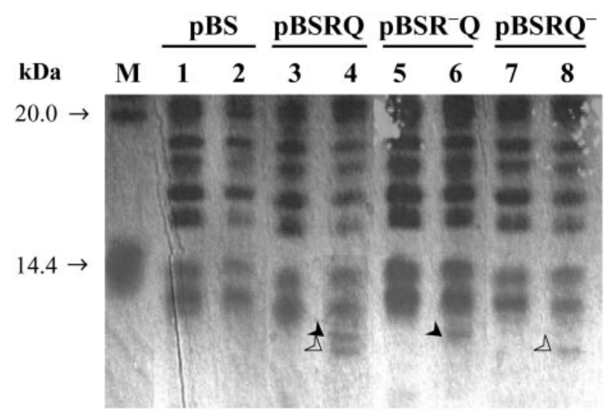

FIG. 4. **SrnR and SrnQ expressed using *E. coli lac* promoter.** *E. coli* having pBS (*lanes 1* and *2*), pBSRQ (*lanes 3* and *4*), pBSR$^-$Q (*lanes 5* and *6*), or pBSRQ$^-$ (*lanes 7* and *8*) were grown in LB broth at 37 °C until A_{600} reached 0.6–0.7 and harvested after IPTG (0.1 mM) induction for 2 h. Cells were broken, and total proteins were subject to Tricine-SDS-PAGE. Induced samples were loaded in *lanes 2*, *4*, *6*, and *8*, whereas non-induced samples were in *lanes 1*, *3*, *5*, and *7*. Molecular mass markers (*lane M*) are indicated with *arrows* to the *left* of the gel. SrnR and SrnQ were marked with *open* and *closed arrowheads*, respectively.

SrnR (12,343 Da) and SrnQ (12,486 Da). We did not believe that *E. coli* RNA polymerase(s) recognized the promoter for *srnR* and *srnQ*, because the polypeptides were not expressed when *srnRQ* were oriented in opposite direction to the plasmid *lac* promoter (data not shown).

Multicopy Effect of srnR and srnQ on FeZn-SOD Expression Is Exerted at the Transcriptional Stage through the sodF Operator—It was determined whether the effects of *srnR* and *srnQ* in multicopies shown above was exerted at the level of *sodF* transcription, and if so, whether the *sodF* operator was involved. The *sodF*::*xylE* fusion plasmids, pIJK365 (the wild-type operator) (Fig. 5) and pIMin(+8+9) (the mutated operator) (Fig. 5), were derived from pXE4, so that they can be compatible with pFD666 or its derivative, pFDRQ. The intro-

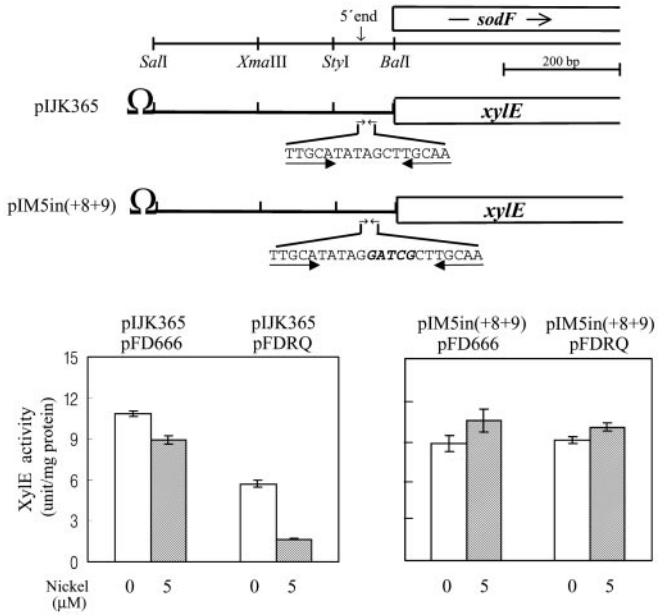

FIG. 5. **Catechol dioxygenase activity of *sodF*::*xylE* transcriptional fusions containing either wild-type (*left panel*) and the mutated operator (*right panel*) with concurrent presence of *srnR* and *srnQ in trans* in *S. griseus*.** Plasmid pIJK365 contained the 365-bp upstream DNA from the 5′ end of *sodF* mRNA. A transcription-translation stop Ω DNA (Sm^r/Sp^r) (22) was cloned at the border between vector and *sodF* DNA. The *sodF* operator of pIM5in(+8+9) had the insertion of GATCG between +8 and +9. Either pFDRQ or pFD666 was transformed into cells, which had harbored either pIJK365 (*left panel*) or pIM5in(+8+9) (*right panel*), and transformants were grown on YEME agar plate for 48 h in the absence (*open bar*) or presence (*shaded bar*) of 5 μM nickel. The mean ± S.D. of activities are shown on each bar.

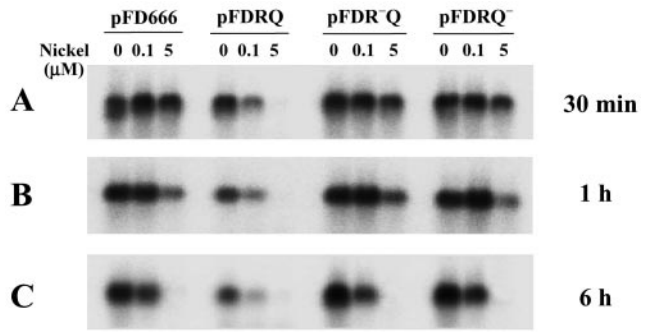

FIG. 6. **Northern (RNA) hybridization analysis of *sodF* transcript of *S. griseus* containing *srnR* and *srnQ in trans*.** *S. griseus* harboring pFD666, pFDRQ, pFDR⁻Q, or pFDRQ⁻ were grown in YEME broth until cell growth reached exponential phase (A_{600} = 0.3). Total RNA was extracted from the cells harvested at 30 min (*A*), 1 h (*B*), and 6 h (*C*) after treatment of culture with nickel (0, 0.1, or 5 μM). The *sodF* transcript (0.8 kb) was hybridized with RNA probe spanning the gene and its 256-bp upstream DNA (11).

duction of pFDRQ into cells, which had harbored pIJK365 (Fig. 5, *left panel*), reduced ~72% XylE activity in the presence of nickel (5 μM) compared with that without nickel addition, whereas the vector DNA pFD666 (Fig. 5, *left panel*) resulted in only 14% decrease of activity in the same comparison. The result suggested that the nickel-responsive repression by *srnR* and *srnQ* in multicopies is regulated at the level of *sodF* transcription. Even without nickel addition, pFDRQ lowered activity (Fig. 5, *left panel, Nickel 0*), which was interpreted as being due to the effect of overexpressed SrnR and SrnQ interacting with the residual nickel in YEME medium. On the other hand, pIM5in(+8+9) did not show any nickel-responsive repression by the presence of pFDRQ (Fig. 5, *right panel*). The results indicated that the enhanced repression by *srnRQ* in multicopies should be exerted through the *sodF* operator.

The nickel-dependent repression by pFDRQ was further confirmed by analyzing the transcription of chromosomal *sodF*. *S. griseus* containing pFDRQ, pFDR⁻Q, and pFDRQ⁻ were grown in YEME broth until exponential phase (A_{600} = 0.3), and nickel was added up to 0.1 or 5 μM. Cells were harvested at times indicated and analyzed for the *sodF* transcript (Fig. 6). The transcript level was largely decreased at 0.1 μM nickel and barely detectable at 5 μM nickel when pFDRQ was contained *in trans*. The reduction of the transcript level by pFDRQ was also observed without nickel addition, which is consistent with the lower XylE activity of pIJK365 in the presence of pFDRQ (Fig. 5, *left panel*, *Nickel 0*). The nickel-responsive repression by pFDR⁻Q and pFDRQ⁻ was not much different from that shown by pFD666 (Fig. 6). In addition, the half-life of *sodF* transcript of the cells containing pFD666 was ~13 min irrespective of the nickel treatment, which was not changed at all by the presence of *srnR* and *srnQ* (data not shown). Thus, *srnRQ* in multicopies highly repressed the *sodF* transcription in a nickel-dependent way.

Chromosomal Interruption of srnR Resulted in Derepressed Transcription of sodF Even in the Presence of Nickel—The chromosomal copy of *srnR* was interrupted with transcription-translation stop Ω DNA (Km^r) (28) to confirm the *in vivo* effects of overexpressed SrnR and SrnQ. The interruption at *Eco*NI site of *srnR* (Fig. 7*A*), we believe, also resulted in a lack of *srnQ* expression because no XylE activity was observed with *S. griseus* containing *srnQ*::*xylE* fusion construct with its 5′-DNA limited to the *Eco*NI site (data not shown), illustrating the dependence of *srnQ* expression on the regulatory DNA upstream from *srnR*. The genomic Southern analysis of *srnR*-interrupted mutant R45 (Fig. 7*A*) revealed the presence of 3.7-kb *Bam*HI bands hybridized to both *srnR* (Fig. 7*B*, *left panel*) and the Ω DNA (Fig. 7*B*, *right panel*), confirming the correct arrangement of chromosomal interruption. Mutant R45 showed the FeZn-SOD activities and *sodF* transcription (Fig. 7, *C* and *D*, respectively), which were no longer repressed by nickel. As expected, the mutation phenotype was complemented only when pFDRQ (Fig. 2) was introduced into R45 (data not shown). The results were consistent with the observed effects by overexpressed SrnR and SrnQ.

Nickel-dependent Binding of SrnR and SrnQ to the sodF Operator Was Observed Only When Both Proteins Were Provided—SrnR and SrnQ were overexpressed as GST fusion proteins and purified from *E. coli* as described under "Experimental Procedures." The purified SrnR and SrnQ showed a molecular mass of ~12 kDa that were identified by SDS-PAGE (data not shown). The 113-bp *Sty*I-*Bal*I (Fig. 5) DNA containing either wild-type sequence (Fig. 8*A*) or the mutated operator (Fig. 8*B*, *+5 insertion*) was used for gel-mobility shift assay. The wild-type DNA was retarded only when SrnR and SrnQ were provided together in the nickel-containing reaction mixture. The retarded band was intensified as nickel concentration increased (Fig. 8*A*). However, neither SrnR nor SrnQ alone shifted the DNA, even in the presence of nickel (Fig. 8*A*). On the other hand, the DNA including the mutated operator did not show any retardation (Fig. 8*B*), being consistent with the XylE activities of pIM5in(+8+9) shown in Fig. 5. Thus, SrnR and SrnQ appear to exert the repressive effect in a nickel-responsive way through binding to the operator. Because SrnR has a DNA binding motif, it is expected that SrnR may directly interact with the operator. However, SrnQ should be present together for the repression.

The gel-mobility shift of the operator DNA was examined with the two proteins in different ratios. No retardation was

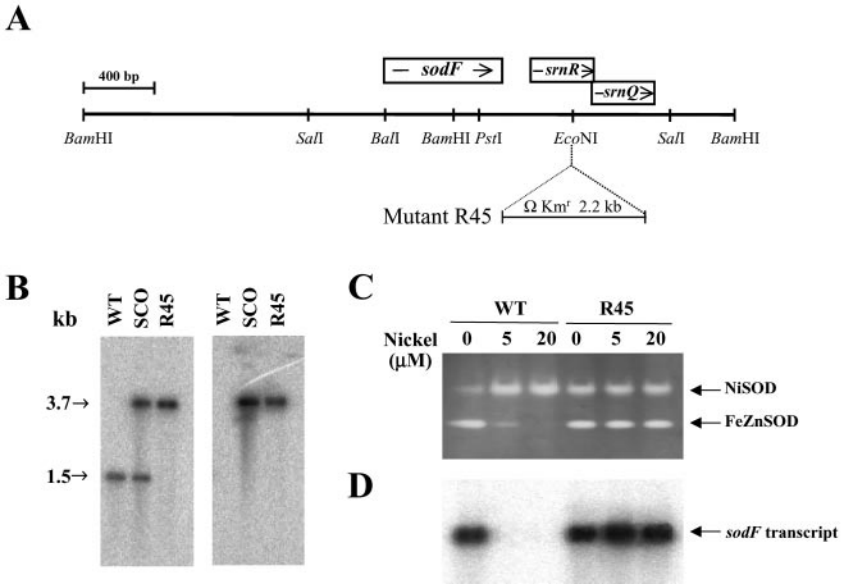

FIG. 7. **Characterization of *srnR* disruptant R45.** *A*, chromosomal disruption of *srnR* by Ω transcription-translation stop DNA (Km^r) (28). *B*, genomic Southern hybridization analysis of R45 and single cross-over (*SCO*) recombinant for comparison with wild type (*WT*). The chromosomal DNA was digested with *Bam*HI and probed with PCR-amplified *srnR* DNA (*left panel*) or probed with 2.2-kb transcription-translation stop Ω DNA (Km^r) (*right panel*). *C*, the extracts from wild-type and R45 mutant, which had been grown in the presence of nickel (0, 5, or 20 μM), were used for the activity staining of SOD as described in Fig. 2. *D*, Northern (RNA) hybridization analysis of *sodF* transcript of wild type and R45. Total RNA was isolated from the cells harvested at 6 h after treatment of culture with nickel (0, 5, or 20 μM). The same RNA probe as used in Fig. 6 was used.

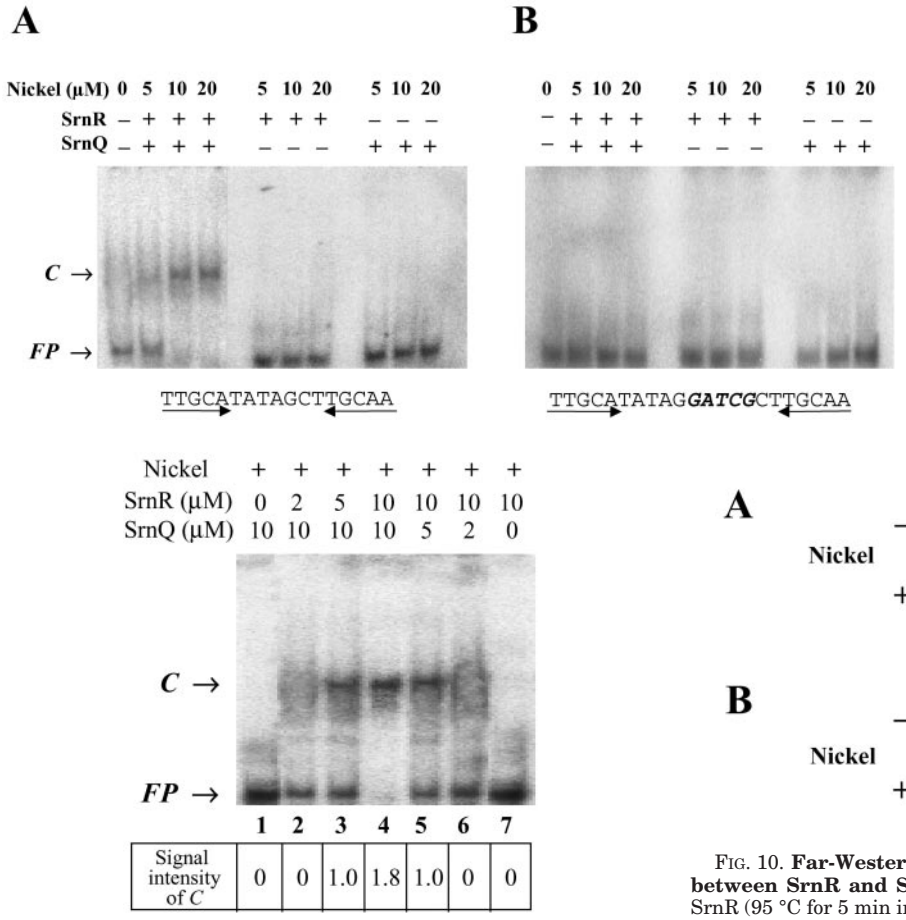

FIG. 9. **Gel-mobility shift assay of the *sodF* regulatory DNA with SrnR and SrnQ in varying amounts.** The wild-type DNA as used in Fig. 8 was incubated with the proteins in the presence of 20 μM nickel. The micromolar ratios of SrnR to SrnQ were 0:10 (*lane 1*), 2:10 (*lane 2*), 5:10 (*lane 3*), 10:10 (*lane 4*), 10:5 (*lane 5*), 10:2 (*lane 6*), and 10:0 (*lane 7*). Free probe (*FP*) and retarded complex (*C*) were indicated with *arrows*. The relative levels of *C* were quantified by densitometer scan of the resulting autoradiogram.

FIG. 8. **Gel-mobility shift assay of *sodF* regulatory DNA (113-bp *Sty*I/*Bal*I in Fig. 5) with purified SrnR and SrnQ.** Wild-type and mutated sequence of *sodF* operator are indicated below the gel. The mutated *Sty*I/*Bal*I DNA was prepared from pIM5in(+8+9). Reaction mixtures containing 400 pmol (10 μM) of SrnR and/or SrnQ were incubated in the absence or presence of nickel (5, 10, and 20 μM). Wild-type DNA (*A*) or mutated DNA (*B*) was used as a probe. Free probe (*FP*) and binding complex (*C*) were indicated with *arrows*.

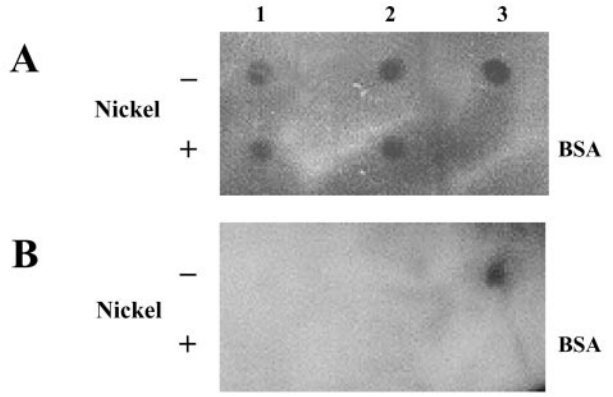

FIG. 10. **Far-Western immunoblot analysis for the interaction between SrnR and SrnQ.** Native SrnR (*panel A*) or the denatured SrnR (95 °C for 5 min in 0.2% SDS) (*panel B*) in TDGT buffer (32) were spotted onto nitrocellulose membrane in the absence (*Nickel* –) or the presence (*Nickel* +) of nickel. The nickel concentration was twice as much as the protein concentration. *Spots 1* contained 2 pmol of SrnR, whereas *spots 2* and *3* had 5 pmol of the proteins. The blots were incubated with native SrnQ (15 nM) followed by reaction with anti-SrnQ antiserum. Native and denatured SrnQ (*panels A* and *B*, *spots 3*, respectively) were used as positive controls, whereas the native and denatured bovine serum albumin (*panels A* and *B*, *BSA*, respectively) were included as negative controls. *BSA*, bovine serum albumin.

consistently observed in the absence of one of the two proteins (Fig. 9, *lanes 1* and *7*). The amount of the binding complex reached the maximum level when SrnR and SrnQ were provided simultaneously at 10 μM each (*lane 4*). The signal intensity of the binding complex (*C*) was ~2-fold higher than that of *lanes 3* and *5* in which one of the two proteins was maintained at half-concentration (5 μM). Thus, the maximum interaction of

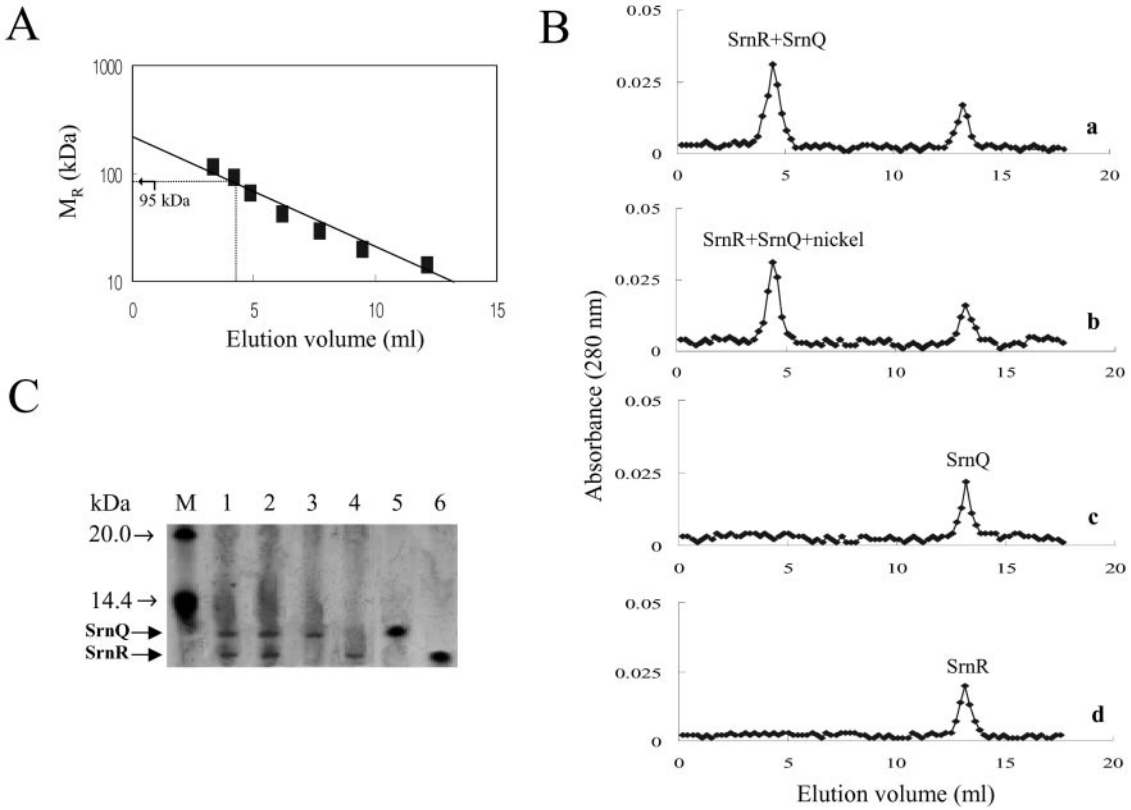

FIG. 11. **Analysis of SrnR·SrnQ complex using gel-filtration chromatography.** *A*, the mass calibration curve for Sephadex G-100 column (1.2 × 20.0, inner diameter × height (in cm)) was drawn with the standard proteins including aldolase (117 kDa), phosphorylase b (94 kDa), albumin (67 kDa), ovalbumin (43 kDa), carbonic anhydrase (30 kDa), trypsin inhibitor (20.1 kDa), and α-lactalbumin (14.4 kDa). *B*, SrnR and SrnQ (60 μg each, 15 μM) were incubated without (*a*) or with (*b*) 20 μM nickel for 10 min and were subjected to the chromatography. Each of SrnQ (*c*) and SrnR (*d*) (40 μg each, 10 μM) was loaded as controls. *C*, the fractions for peaks were analyzed using Tricine-SDS-PAGE. The fractions (10 μg each) pooled for the 95-kDa peaks without or with nickel (*panel B*, *a* and *b*) were included in *lanes 1* and *2*, respectively, whereas the peak fractions (5 μg each) for SrnQ (*Panel B*, *c*) and SrnR (*Panel B*, *d*) were loaded in *lanes 3* and *4*, respectively. 50 μg of the purified SrnQ (*lane 5*) and SrnQ (*lane 6*) were included as controls. The molecular mass markers (*lane M*) are shown to the *left*.

SrnR and SrnQ to the *sodF* operator appears to require both proteins in 1:1 ratio.

SrnR and SrnQ Directly Interact with Each Other, and the Interaction Does Not Require Nickel—Both native (Fig. 10*A*, *spots 1* and *2*) and SDS-heat-denatured SrnR (Fig. 10*B*, *spots 1* and *2*) were spotted on nitrocellulose membrane, and the blots were incubated with native SrnQ followed by treatment with anti-SrnQ mouse antiserum, which was then detected using anti-mouse IgG conjugated with horseradish peroxidase. The two proteins in native forms interact with each other by direct binding, even in the absence of nickel (Fig. 10*A*, *Nickel−*, *spots 1* and *2*). Indifference in signal intensity between the applications of 2 and 5 pmol (*spots 1* and *2*, respectively) of SrnR onto the membrane was probably attributed to the limiting concentration of SrnQ (15 nM) used in binding. Denatured SrnR did not interact with SrnQ irrespective of nickel treatment (Fig. 10*B*, *spots 1* and *2*). The control immunoblots with SrnQ in native and SDS-heat-denatured forms showed positive signals by anti-SrnQ antiserum as expected (Fig. 10, *A* and *B*, *spots 3*, respectively). Bovine serum albumin did not show any reaction (Fig. 10, *A* and *B*, *BSA*), and no cross-reactivity was observed between SrnR and anti-SrnQ antiserum (data not shown). The analyses with SrnQ on the membrane followed by sequential reactions with SrnR, anti-SrnR antiserum, and anti-mouse IgG-horseradish peroxidase displayed the same results (data not shown). From the results, it was evident that the interaction between the two proteins does not require nickel and that the protein-protein interaction can take place before binding to the operator DNA.

SrnR and SrnQ Constitute a Hetero-octameric Complex Composed of Each Protein in 1:1 Ratio—The formation of SrnR·SrnQ complex was confirmed through gel-filtration chromatography of Sephadex G-100, and its molecular weight was measured using the mass calibration curve drawn with the standard proteins (Fig. 11*A*). The chromatographic resolution of either SrnR or SrnQ alone showed a peak, which was estimated around 10–12 kDa (Fig. 11*B*, *c* and *d*). Nickel treatment to each protein prior to gel loading showed the same results (data not shown), which implied that SrnR or SrnQ by itself, does not form homomultimeric complex. The two proteins were incubated with or without nickel and then subjected to the column chromatography. The elution profiles revealed an identical peak corresponding to ~95 kDa regardless of the nickel treatment (Fig. 11*B*, *a* and *b*). The Tricine-SDS-PAGE of the 95-kDa fractions showed the two protein bands with equal intensity, which co-migrated with SrnR and SrnQ (Fig. 11*C*). Thus, SrnR and SrnQ appear to form an octameric complex composed of four subunits of each protein.

Nickel Binds to SrnQ—The CD spectra of SrnQ were largely changed after nickel treatment (Fig. 12*A, left panel*). However, the spectral patterns of SrnR did not show any significant difference with respect to nickel (Fig. 12*A, right panel*). The spectral change of SrnQ by nickel disappeared following incubation of the protein mixture with EDTA (50 mM) for 3 h at room temperature (data not shown). The results suggested that the nickel binding to SrnQ causes the conformational change of the protein.

Atomic absorption spectrophotometry of SrnQ following equilibrium dialysis against nickel showed the metal-binding

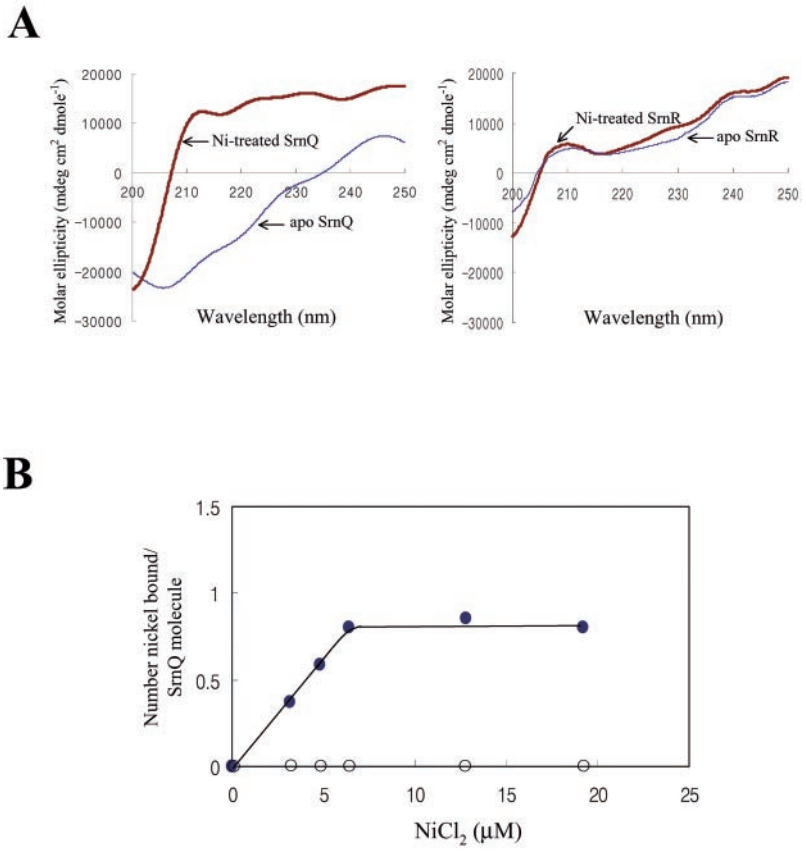

FIG. 12. **Nickel binding to SrnQ.** *A*, CD spectra of SrnQ (*left panel*) and SrnR (*right panel*) treated with or without nickel (20 μM). Proteins were used at 15 μM. *B*, nickel-binding saturation curve of SrnQ (6.4 μM). Nickel binding was determined by equilibrium dialysis against varying concentrations of nickel followed by atomic absorption spectrophotometry. ●, SrnQ; ○, bovine serum albumin (negative control).

capacity of the protein that saturates at ~0.80 atom of nickel/molecule with an apparent K_d of 0.65 μM. Thus, the stoichiometric balance of at least 1:1 is expected for Ni^{2+} ion bound to SrnQ. Other metals such as Zn^{2+} and Cd^{2+} were found in the ratio <0.04 metal atom/protein molecule, and no binding signal was detected with other metal ions including Ca^{2+}, Mg^{2+}, Cu^{2+}, Mn^{2+}, and Co^{2+} (data not shown). In addition, SrnR did not reveal any metal-binding capacity (data not shown). Thus, the nickel specifically binds to SrnQ, which appears to be in a stoichiometric balance of 1:1 (Ni^{2+}/SrnQ).

DISCUSSION

A highly aerobic organism, *S. griseus* contains Ni-SOD and FeZn-SOD for protection against oxidative damages by superoxide radicals. Ni-SOD activity increased after nickel treatment,[2] whereas FeZn-SOD expression is repressed by nickel at the stage of transcription (10, 11). The transcriptional repression was exerted through an operator of *sodF* (11). The antagonistic production of the two SODs has been proposed as a regulatory circuit to keep the total SOD activity constant (10). In this work, we found two ORFs, SrnR and SrnQ, which are responsible for the nickel-responsive transcriptional repression of *S. griseus sodF*. When SrnR and SrnQ were maintained in multicopies in *S. griseus*, the Ni-SOD activity was not changed much, indicating that *sodN* expression is regulated differently from that of *sodF*.

The calculated pI of SrnQ, fairly rich (26%) in arginine, is 12.8, whereas that of SrnR is 7.0. The physiological implication of the basic pI of SrnQ is not known. The constitutive expression of *srnRQ* independent of the presence of nickel was identified using *srnR*::*xylE* transcriptional fusion construct.[2] This result explains the observation that the binding complex with the *sodF* operator DNA was still detected in gel-mobility shift assay when nickel was added to the cell extracts prepared from a nickel-deficient culture of *S. griseus*.[2]

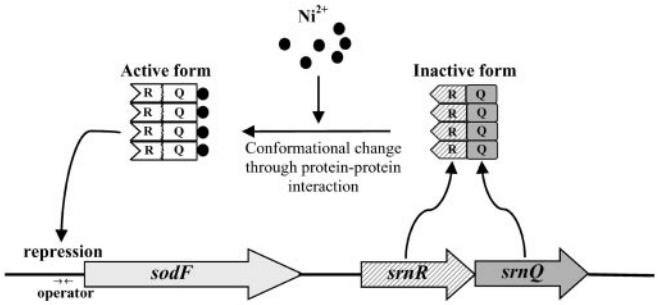

FIG. 13. **A model illustrating nickel-dependent repression of *sodF* transcription by the complex of SrnR·SrnQ.** The *sodF* operator was indicated with facing *arrows* (11). Nickel ion was shown as *closed circles*. *R* and *Q* denote SrnR and SrnQ, respectively.

The gel-mobility shift band (Fig. 8) was compared with those observed with the cell extracts of *S. griseus*. The retarded band with the purified proteins exactly co-migrated with one (faster-moving band) of the two binding complexes with the cell extracts (11). The slower-moving band was not detected, even with up to five times more the amount of the purified proteins shown in Fig. 8,[2] so the band might reflect additional binding of other proteins from cell extracts. The probe DNA contains the *sodF* promoter as well.

The results shown in this work clearly suggest that SrnR interacts with SrnQ to form an octameric complex, which appears to be composed of four subunits of each protein (Fig. 13). The overlapping stop-start codons of SrnR and SrnQ may provide a balanced translation to maintain 1:1 stoichiometry of the two proteins. The protein interaction does not require nickel. Our current data explain that SrnQ of the complex is probably a co-repressor of SrnR, because it can hold nickel at a ratio of one Ni^{2+}/polypeptide and the ligand binding appears to change the conformation of SrnQ, which may in turn enhance the DNA

binding activity of SrnR through the protein-protein interaction. The complex then binds to the *sodF* operator for transcriptional repression (Fig. 13). A similar observation has been reported for the interaction between BarA repressor and BarX co-repressor of *Streptomyces virginiae* (38–40). They are needed together for binding to the operator site of *barB-varS* operon, which codes for a putative DNA-binding protein and virginiamycin *S*-specific transport protein, respectively. BarX was suggested to induce DNA binding ability of BarA by direct interaction.

A nickel-sensing transcriptional repressor NikR of *E. coli* has been reported as a direct sensor of nickel ion to negatively regulate *nikABCDE* expression by binding to an operator consisting of two 5′-GTATGA-3′ half-sites related by dyad symmetry and separated by 16 base pairs (14). Roughly, a one-nickel ion was proposed to bind to each NikR subunit of the acting dimeric complex (41). No homology between the primary structures of SrnR and NikR was found.

Taken together, the experimental results presented here provide an interesting example of transcriptional repression by the protein complex composed of the DNA binding motif-bearing repressor and nickel-binding co-repressor. The detailed nature of the protein-protein interaction between the repressor and co-repressor remains to be determined.

REFERENCES

1. Storz, G., Tartaglia, L. A., Farr, S. B., and Ames, B. N. (1990) *Trends Genet.* **6,** 363–368
2. Cannio, R., Fiorentino, G., Morana, A., Rossi, M., and Bartolucci, S. (2000) *Front. Biosci.* **5,** 768–779
3. Ahmad, S. (1995) in *Oxidative Stress and Antioxidant Defenses in Biology* (Ahmad, S., ed) pp. 238–272, Chapman & Hall, New York, NY
4. Imlay, K. R. C., and Imlay, J. A. (1996) *J. Bacteriol.* **178,** 2564–2571
5. Steinman, H. M. (1985) *J. Bacteriol.* **162,** 1255–1260
6. Steinman, H. M. (1987) *J. Biol. Chem.* **262,** 1882–1887
7. Youn, H.-D., Youn, H., Lee, J.-W., Yim, Y.-I., Lee, J. K., Hah, Y. C., and Kang, S.-O. (1996) *Arch. Biochem. Biophys.* **334,** 341–348
8. Kim, E.-J., Kim, H.-P., Hah, Y. C., and Roe, J.-H. (1996) *Eur. J. Biochem.* **241,** 178–185
9. Kim, E.-J., Chung, H.-J., Suh, B., Hah, Y. C., and Roe, J.-H. (1998) *Mol. Microbiol.* **27,** 187–195
10. Kim, E.-J., Chung, H.-J., Suh, B., Hah, Y. C., and Roe, J.-H. (1998) *J. Bacteriol.* **180,** 2014–2020
11. Kim, J.-S., Jang, J.-H., Lee, J.-W., Kang, S.-O., Kim, K.-S., and Lee, J. K. (2000) *Biochim. Biophys. Acta.* **1493,** 200–207
12. Navarro, C., Wu, L.-F., and Mandrand-Berthelot, M.-A. (1993) *Mol. Microbiol.* **9,** 1181–1191
13. de Pina, K., Desjardin, V., Mandrand-Berthelot, M.-A., Giordano, G., and We, L.-F. (1999) *J. Bacteriol.* **181,** 670–674
14. Chivers, P. T., and Sauer, R. T. (2000) *J. Biol. Chem.* **275,** 19735–19741
15. Hopwood, D. A., Bibb, M. J., Chater, K. F., Kieser, T., Bruton, C. J., Kieser, H. M., Lydiate, D. J., Smith, C. P., and Ward, J. M. (1985) *Genetic Manipulation of Streptomyces: A Laboratory Manual*, pp. 69–247, The John Innes Foundation, Norwich, CT
16. Ohnishi, Y., Kameyama, S., Onaka, H., and Horinouchi, S. (1999) *Mol. Microbiol.* **34,** 102–111
17. Oh, S.-H., and Chater, K. F. (1997) *J. Bacteriol.* **179,** 122–127
18. Greener, A. (1990) *Strategies* **5,** 81–83
19. McPherson, M. J. (1991) *Directed Mutagenesis: A Practical Approach*, Oxford University Press, NY
20. Denis, F., and Brzezinski, R. (1992) *Gene* (*Amst.*) **111,** 115–118
21. Ingram, C., Brawner, M., Youngman, P., and Westpheling, J. (1989) *J. Bacteriol.* **171,** 6617–6624
22. Prentki, P., and Krisch, H. M. (1984) *Gene* (*Amst.*) **29,** 303–313
23. Beauchamp, C., and Fridovich, I. (1971) *Anal. Biochem.* **44,** 276–287
24. Sambrook, J., and Russell, D. W. (2001) *Molecular Cloning: A Laboratory Manual*, 3rd Ed., Cold Spring Harbor Laboratory, Cold Spring Harbor, NY
25. Markwell, M. A., Haas, S. M., Bieber, L. L., and Tolbert, N. E. (1978) *Anal. Biochem.* **87,** 206–210
26. Schägger, H., and von Jagow, G. (1987) *Anal. Biochem.* **166,** 368–379
27. Bierman, M., Logan, R., O'Brien, K., Seno, E. T., Nagaraja Rao, R., and Schoner, B. E. (1992) *Gene* (*Amst.*) **116,** 43–49
28. Eraso, J. M., and Kaplan, S. (1994) *Microbiology* **141,** 1805–1819
29. Horinouchi, S., Suzuki, H., and Beppu, T. (1986) *J. Bacteriol.* **168,** 257–269
30. DeHoff, B. S., Lee, J. K., Donohue, T. J., Gumport, R. I., and Kaplan, S. (1988) *J. Bacteriol.* **170,** 4681–4692
31. Retzlaff, L., and Distler, J. (1995) *Mol. Microbiol.* **18,** 151–162
32. Luo, Z.-Q., Qin, Y., and Farrand, S. K. (2000) *J. Biol. Chem.* **275,** 7713–7722
33. Dempsey, B. R., Economou, A., Dunn, S. D., and Shilton, B. H. (2002) *J. Mol. Biol.* **315,** 831–843
34. Williams, S. G., Attridge, S. R., and Manning, P. A. (1993) *Mol. Microbiol.* **9,** 751–760
35. Rosenstein, R., Peschel, A., Wieland, B., and Götz, F. (1992) *J. Bacteriol.* **174,** 3676–3683
36. Kondorosi, E., Pierre, M., Cren, M., Haumann, U., Buiré, M., Hoffmann, B., Schell, J., and Kondorosi, A. (1991) *J. Mol. Biol.* **222,** 885–896
37. Sedlmeier, R., and Altenbuchner, J. (1992) *Mol. Gen. Genet.* **236,** 76–85
38. Kinoshita, H., Ipposhi, H., Okamoto, S., Nakano, H., Nihira, T., and Yamada, Y. (1997) *J. Bacteriol.* **179,** 6986–6993
39. Lee, C.-K., Kamitani, Y., Nihira, T., and Yamada, Y. (1999) *J. Bacteriol.* **181,** 3293–3297
40. Kawachi, R., Akashi, T., Kamitani, Y., Sy, A., Wangchaisoonthorn, U., Nihira, T., and Yamada, Y. (2000) *Mol. Microbiol.* **36,** 302–313
41. Chivers, P. T., and Sauer, R. T. (1999) *Protein Sci.* **8,** 2494–2500